Electrodeposition of Gold Particles on Aluminum Substrates Containing Copper

Tim S. Olson, Plamen Atanassov, and Dmitri A. Brevnov*

Department of Chemical and Nuclear Engineering, Center for Micro-Engineered Materials, The University of New Mexico, Albuquerque, New Mexico 87131

Received: September 23, 2004; In Final Form: November 1, 2004

Electrodeposition of adhesive metal films on aluminum is traditionally preceded by the zincate process, which activates the aluminum surface. This paper presents an alternative approach for activation of aluminum by using films containing 99.5% aluminum and 0.5% copper. Aluminum/copper films are made amenable for subsequent electrodeposition by anodization followed by chemical etching of aluminum oxide. The electrodeposition of gold is monitored with electrochemical impedance spectroscopy (EIS). Analysis of EIS data suggests that electrodeposition of gold increases the interfacial capacitance from values typical for electrodes with thin oxide layers to values typical for metal electrodes. Scanning electron microscopy examination of aluminum/copper films following gold electrodeposition shows the presence of gold particles with densities of 10^5-10^7 particles cm^{-2}. The relative standard deviation of mean particle diameters is approximately 25%. Evaluation of the micrographs suggests that the electrodeposition occurs by instantaneous nucleation followed by growth of three-dimensional semispherical particles. The gold particles, which are electrically connected to the conductive aluminum/copper film, support a reversible faradaic process for a soluble redox couple. The deposited gold particles are suitable for subsequent metallization of aluminum and fabrication of particle-type films with interesting catalytic, electrical, and optical properties.

Introduction

The surface of aluminum metal is spontaneously oxidized in the ambient atmosphere. This oxidation creates a highly resistive film of native aluminum oxide, which has an adverse effect on electrodeposition of metals (e.g., Ni, Ag, and Cu).[1,2] To overcome this problem, the zincate process is employed in industry for the deposition of adhesive metallic films on aluminum.[1−5] The process consists of immersing the aluminum substrate in a strong alkaline zincate solution. The native aluminum oxide is dissolved, and zinc is deposited on the surface via galvanic displacement by aluminum. As a result, the zinc-coated aluminum surface becomes amenable for electrodeposition of adhesive layers of metals, including nickel[6,7] and copper.[2] Zincate surface activation of aluminum has proven to be a cost-effective process for nickel bumping of wafers prior to flip-chip assembly.[6,7]

Regardless of the universal acceptance of the zincate process in commercial applications, there are incentives for developing alternative methods for the electrodeposition of metals on aluminum. Other procedures for plating on aluminum were suggested because the zincate method is sensitive to many variables. For example, direct electrodeposition of copper on aluminum was reported for several copper complexes.[8] A plating procedure for nickel displacement of aluminum followed by electroless nickel deposition was also discussed.[7] In addition, an organic solvent was used to lay a seed layer of copper or palladium on aluminum substrates. Then, electroless deposition with a reducing agent was utilized to deposit substantially more copper.[9] Recently, we reported a procedure for electroless deposition of silver on films containing 99.5% aluminum and 0.5% copper.[10] These results prompted us to explore the possibilities of electrodeposition of other noble metals on aluminum/copper substrates. In this paper, we describe a procedure for the electrodeposition of gold particles on films containing 99.5% aluminum and 0.5% copper.

Electrodeposition of metals on semiconductors and metals covered with a layer of metal oxide generally occurs by the three-dimensional island growth (Volmer−Weber) mechanism.[11−13] This mechanism has been reported for the electrodeposition of Au,[14] Cu,[15] Pt,[12] on Si; Cu on TaN;[16,17] Ag[18] and Pt[19] on the atomically smooth graphite basal plane surface; Ag and Au on Si;[20] Tl, Cd, and Cu on Si;[21] and Pt on oxidized Ti.[22] Electrodeposition has been shown to follow the models for either instantaneous or progressive nucleation.[23−28] If nucleation is fast and is separated in time from growth of particles, then nucleation is considered to be instantaneous. In this case, following the onset of deposition, the number of particles remains constant. On the other hand, if nucleation is slow and coincides in time with growth of particles, nucleation is considered to be progressive. In contrast to the instantaneous nucleation case, the number of particles continuously increases during deposition. For both models, the growth of particles can proceed under kinetic, diffusion, or mixed control.

In addition to being useful for metallization of the aluminum surface, electrodeposition of noble metals on aluminum has a variety of potential applications. For example, gold nanoparticles deposited on solid supports exhibit useful catalytic and electrocatalytic properties.[29−32] Moreover, the catalytic activity of gold nanoparticles exhibits significant size dependence.[33] Gold nanoparticles with diameters of less than 4 nm have been shown to be an efficient catalyst for CO oxidation.[34,35] A significant positive shift was reported for two cathodic peaks associated with oxygen reduction by gold particles electrodeposited on glassy carbon electrodes.[36] In addition, composite materials with gold nanoparticles are known to have interesting electrical and optical properties[37,38] and tunable surface plasmon resonances.[39]

* Corresponding author. E-mail: dbrevnov@unm.edu.

10.1021/jp045670w CCC: $30.25
Published on Web 12/29/2004

The first objective of this study is to develop a new method for the pretreatment of aluminum surfaces that makes them amenable for the electrodeposition of gold. This objective can be achieved by alloying aluminum with copper, anodizing, and then chemically etching aluminum oxide. The second objective is to investigate the mechanism of electrodeposition of gold particles on aluminum/copper substrates. A combination of electrochemical measurements and scanning electron microscopy (SEM) allows us to discriminate whether electrodeposition occurs by instantaneous or progressive nucleation. The third objective is to show that the electrodeposited gold particles are electrically connected to the aluminum/copper substrate and can be utilized for electroanalytical applications. This objective is accomplished by examining the electron transfer between the aluminum/copper film with gold particles and a soluble redox couple.

Experimental Section

The aluminum/copper wafers used in this study were fabricated as follows: First, a 600-nm layer of SiO_2 was thermally grown by steam oxidation of a silicon wafer. Second, a 3-μm layer (99.5 wt % aluminum and 0.5 wt % copper) was deposited on the layer of SiO_2 by physical vapor deposition (PVD). These steps were performed at Sandia National Laboratories (Albuquerque, NM). Third, the wafer was anodized in an electrochemical cell at 50 V dc for 20 min in 3% w/v oxalic acid at 0 °C. Fourth, the porous and barrier aluminum oxide layers were chemically etched in a solution of 0.4 M phosphoric acid and 0.2 M chromic acid at 60 °C for approximately 2 h. Precautions were taken to avoid Ag^+ contamination in the electrochemical cell during etching because silver can be deposited on aluminum/copper films by galvanic displacement.[10] Fifth, gold electrodeposition was carried out at room temperature (22 °C) in 1.0 M Na_2SO_3 (pH 8) with the Technic Inc. Oromerse Part B gold plating solution. The final concentration of $Na_3Au(S_2O_3)_2$ was 4.3 mM.

Anodization of aluminum/copper films was carried out with a platinum mesh counter electrode and a Hewlett-Packard 4140B pA meter/dc voltage source. Electrodeposition, cyclic voltammetry (CV), and electrochemical impedance spectroscopy (EIS) were performed in a three-electrode cell with the same platinum counter electrode and either a platinum wire (quasireference) or Ag/AgCl reference electrode. All experiments were performed with an IM6-e impedance measurement unit (BAS-Zahner). EIS data were acquired at open-circuit potential (OCP) over a frequency range between 1 Hz and 100 kHz with an AC potential amplitude of 5 mV and were normalized to the electrode geometric area of 1.4 cm^2. The surface morphology of deposited gold was evaluated with a Hitachi (S-5200) scanning electron microscope equipped with a PGT spectrometer for energy-dispersive spectroscopy (EDS). The microscope was operated at 10 kV for imaging and at 25 kV for EDS. In the body of this paper, the term "processed" wafer refers to a silicon wafer with an aluminum/copper film that has been anodized and etched, whereas the phrase "unprocessed" wafer refers to a silicon wafer with an aluminum/copper film that has not been anodized and etched.

Results and Discussion

Films composed of 99.5% aluminum and 0.5% copper were anodized and chemically etched to activate the aluminum surface for subsequent electrodeposition of gold. Whereas anodization forms both barrier and porous aluminum oxide layers, etching results in complete dissolution of porous aluminum oxide and partial dissolution of barrier aluminum oxide. Figure 1 shows the current−potential curves collected under anaerobic conditions for three substrates: two with $Na_3Au(S_2O_3)_2$, (a) processed wafer and (c) unprocessed wafer, and one without $Na_3Au(S_2O_3)_2$, (b) processed wafer. Evaluation of collected current−potential curves results in the following conclusions. First, a comparison of curves a and b suggests that an excess of cathodic current for curve a at sufficiently negative potentials corresponds to the reduction of $Na_3Au(S_2O_3)_2$ and the concurrent deposition of gold metal. Second, evaluation of curves a and c indicates that the cathodic current that corresponds to electrodeposition of gold is significantly more pronounced for the processed wafer. Third, current−potential curve a shows no peak on the reverse scan; thus, the reduction of $Na_3Au(S_2O_3)_2$ is irreversible process. Fourth, the cathodic current for curve a increases in exponential fashion over the investigated range of overpotentials and shows neither peak nor plateau, which could be attributed to mass-transport limitations. This observation could be explained by an onset of water electrolysis catalyzed by deposited gold.

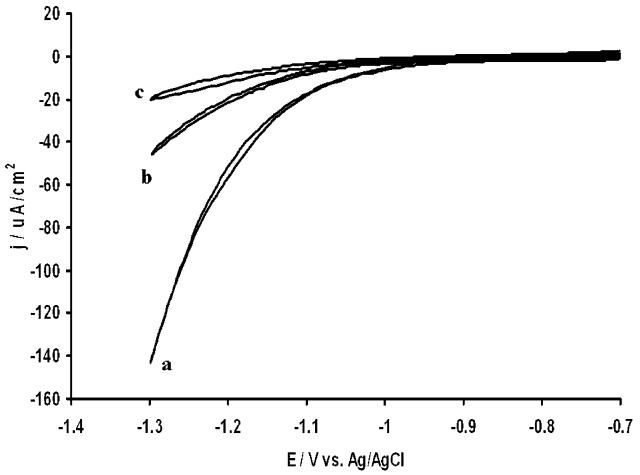

Figure 1. Cyclic voltammograms (100 mV/s) for gold electrodeposition on (a) processed wafer and (c) an unprocessed wafer. Background scan: (b) Processed wafer without gold(I) sodium thiosulfate.

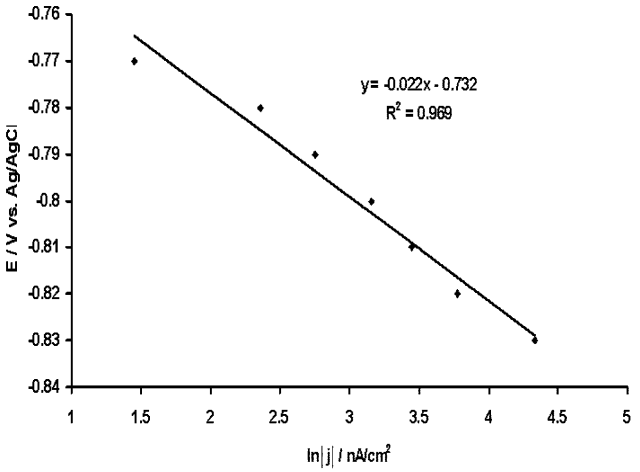

Figure 2. Tafel plot for gold electrodeposition on a processed wafer.

To further characterize the electrodeposition of gold, a Tafel plot (Figure 2) was obtained for potentials up to 60 mV more negative than OCP of the aluminum/copper electrode in the investigated electrolyte (−0.76 V vs Ag/AgCl). This relatively small potential range was chosen to minimize the amount of gold deposited on the substrate during the experiments. The form of the Tafel equation used here is given by[40]

$$E = \text{const} - \frac{RT}{\alpha nF} \ln |j| \qquad (1)$$

where E is the potential, R is the gas constant, T is the absolute temperature, α is the cathodic charge-transfer coefficient, n is the number of electrons, F is the Faraday constant, and j is the current density. The Tafel slope of the shown data (E vs ln $|j|$) is found to be -0.022 V. This value indicates that the reduction of the gold complex in solution is a one-electron process, assuming that α is equal to 1. A slope of -0.026 V is expected from eq 1.[40] The one-electron process corresponds to the following electrochemical reaction

$$Au(S_2O_3)_2^{3-} + e^- \rightarrow Au(s) + 2(S_2O_3)^{2-} \qquad (2)$$

Although the formal potential for the reduction of $Au(S_2O_3)_2^{3-}$ is -0.05 V (Ag/AgCl),[41] significantly more negative potentials of $0.7-0.8$ V are required for gold electrodeposition. These potentials result from two components: a potential drop in the layer of barrier aluminum oxide and a potential drop in the Helmholtz layer.[11,12,17] The latter component includes the nucleation and kinetic overpotentials.

EIS was recently reported to be a useful method for in situ monitoring of the thickness of the layer of barrier aluminum oxide after anodization (step 3 in the Experimental Section) and during chemical etching (step 4 in the Experimental Section).[42] An equivalent circuit (inset in Figure 3) used for modeling of the total cell impedance includes two parallel combinations of a constant phase element (CPE) and a resistor (R) connected in series with each other and the cell uncompensated resistance (R_u). The CPE is frequently used instead of a pure capacitance to describe interfacial dielectric properties. One of two parallel (R_1 CPE_1) combinations is attributed to the layer of barrier aluminum oxide. In this case, CPE_1 describes the dielectric properties of barrier aluminum oxide, and R_1 describes the resistance to ion migration through the barrier aluminum oxide. The second (R_2 CPE_2) combination possibly represents the inner layer of aluminum oxide with different dielectric properties, which is located between the aluminum phase and outer layer of barrier aluminum oxide.[42] The analysis of EIS data allowed us to establish the necessary duration of the etching process (typically $90-120$ min). At the end of the etching process, the layer of barrier aluminum oxide reaches its minimal thickness, which facilitates the electrodeposition process (step 4 in the Experimental Section).

In addition to monitoring of the etching rate of barrier aluminum oxide, EIS can be used as a convenient quality-control method to observe changes in the interfacial electrical properties induced by the electrodeposition of gold particles on the aluminum/copper substrate. Figure 3 depicts a Bode plot for the aluminum/copper film with deposited gold (deposited for approximately 20 min at a current density of -0.018 mA/cm^2). Fitting of the experimental EIS data to the same equivalent circuit allowed us to extract values of the components of the equivalent circuit. For this EIS data set, R_u is 39.9 ± 0.6 Ω, R_1 is 8.7 ± 0.9 kΩ cm^2, CPE_1 is 13.0 ± 0.5 μF s$^{\alpha-1}$/cm^2, α_1 is 0.939 ± 0.001, R_2 is 12.2 ± 0.8 Ω cm^2, CPE_2 is 7.8 ± 0.7 μF s$^{\alpha-1}$/cm^2, and α_2 is 0.812 ± 0.008. To better understand the time dependence of gold electrodeposition on the aluminum/copper films, EIS experiments were carried out according to the following protocol. Galvanostatic electrodeposition (-0.018 mA/cm^2) was preformed over relatively short time intervals (30 s$-$1 min) and was followed by EIS at the OCP. Interruption of galvanostatic electrodeposition was necessary to satisfy one of the requirements for the validity of EIS measurements. The system under investigation is required not to change over the time (about 3 min) necessary to collect an EIS spectrum.

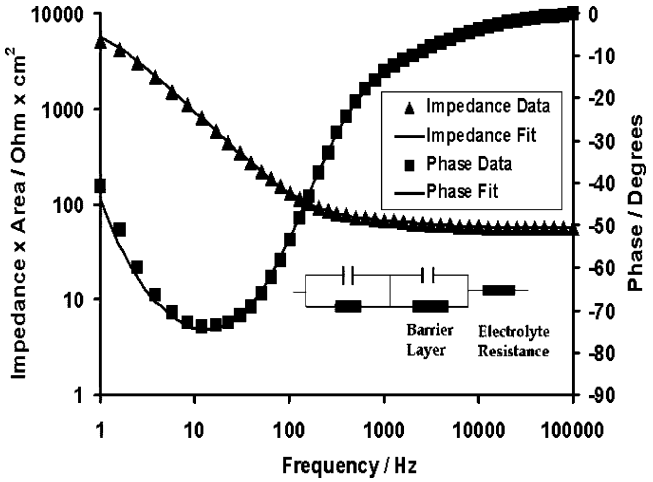

Figure 3. Bode plot (magnitude and phase) after a total of 20 min of galvanostatic gold electrodeposition at -0.018 mA/cm^2 performed for 30- or 60-s intervals. Inset: Equivalent circuit used to model EIS data.

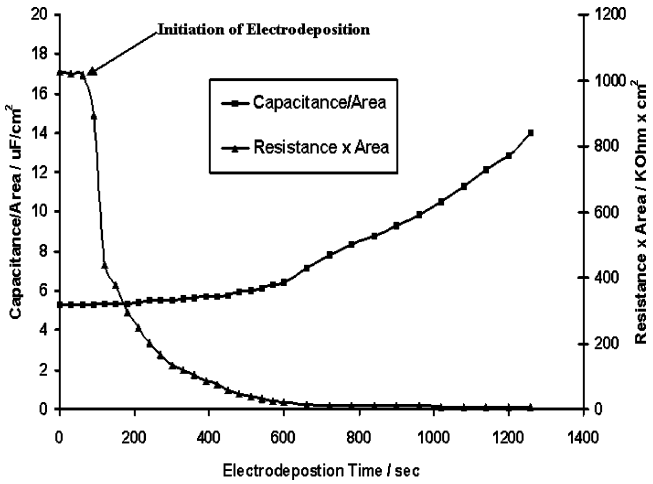

Figure 4. Resistance and capacitance of the first parallel combination (R_1 and CPE_1) as a function of time during galvanostatic electrodeposition (-0.018 mA/cm^2) of gold on a processed wafer.

Figure 4 illustrates the magnitude of CPE_1 and R_1 as a function of deposition time. Over the investigated period of time, CPE_1 monotonically increases from values typical for electrodes with thin oxide layers ($5-6$ μF/cm^2)[42] to values approaching those typical for metal electrodes (20 μF/cm^2).[40] In contrast, the resistance of barrier aluminum oxide (R_1) drops rapidly in the few first minutes of electrodeposition from approximately 1 MΩ cm^2 to 300 kΩ cm^2. Thereafter this resistance gradually decreases to values approaching 10 kΩ cm^2. This observation most likely results from the incorporation of gold in the layer of barrier aluminum oxide and, as a result, an increase in the electronic conductivity in this layer. On the basis of these observations, we conclude that electrodeposition of gold results in the formation of gold particles that directly affect both the interfacial capacitance and resistance. Thus, these particles have an intimate electrical contact to the conductive aluminum/copper substrate. Low resistances are important for the aluminum/copper film with gold particles to be used in electrocatalysis[29,31] and electro-analytical applications.[43] We note that EIS and Tafel data are collected at different time scales. Whereas the time scale for EIS is less than 1 s, the time scale for the Tafel experiment is longer. In addition, the EIS and Tafel data are acquired at significantly different cathodic current densities,

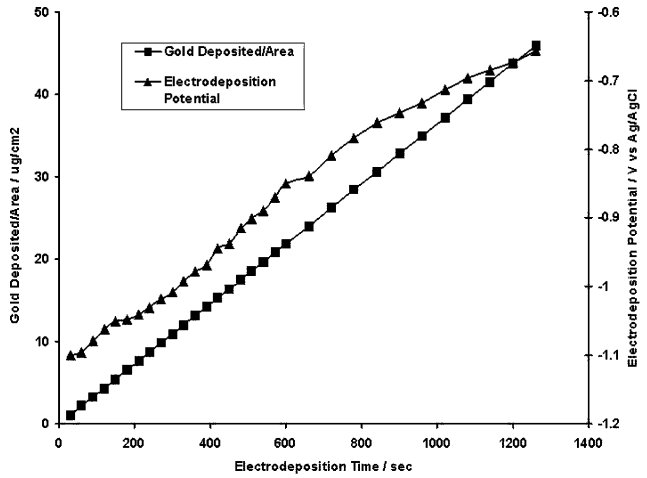

Figure 5. Mass of gold deposited per unit area and electrodeposition potential as a function of electrodeposition time.

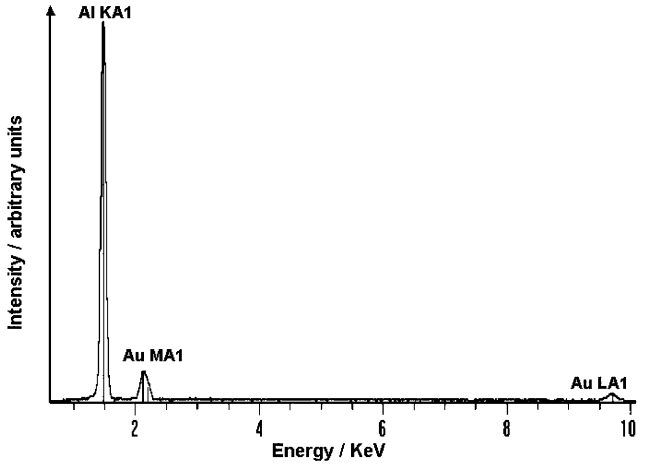

Figure 6. EDS spectrum obtained after 5 min of gold electrodeposition (-0.018 mA/cm^2).

0.018 mA/cm^2 and less than 0.1 μA/cm^2, respectively. Thus, a direct comparison of two data sets related to the resistance of barrier aluminum oxide (R_1) is not possible.

In addition to changes in the interfacial electrical properties, it is worthwhile to note a systematic increase in the deposition potential during galvanostatic deposition (Figure 5). After approximately 23 min of electrodeposition, the potential needed to maintain the same current (-0.018 mA/cm^2) was over 0. 4 V more positive than the initial value of -1.1 V. This observation indicates that the overall overpotential diminishes for sequential electrodeposition intervals. Also shown in Figure 5 is the amount of gold deposited per unit area, which was calculated according to eq 3, assuming ideal conditions for electrodeposition (100% faradaic efficiency)

$$m/A = \left(\frac{jt}{nF}\right)M \times 10^6 \qquad (3)$$

where m is the mass of gold deposited (μg), A is the geometric electrode area (cm^2), t is the electrodeposition time (s), and M is the atomic weight of gold (g/mol). Analysis of Figure 5 suggests that a monotonic increase in the deposition potential correlates with the amount of deposited gold. The deposited particles were also characterized with EDS. Figure 6 shows an EDS spectrum collected after 5 min of gold electrodeposition. The spectrum confirms the presence of both gold and aluminum.

The mechanism of electrodeposition, i.e., nucleation and growth of gold particles, was investigated by generating four samples at two different current densities of -0.54 and -1.1 mA/cm^2 and two electrodeposition times of 10 and 20 s. During these experiments, the electrodeposition potential at which the aluminum/copper electrode was polarized at the end of electrodeposition became only slightly more positive than its initial value. Figures 7 and 8 present micrographs of the aluminum/copper electrodes with deposited gold particles. Histograms shown as insets in Figures 7 and 8 were collected by analyzing low-magnification micrographs. As a result, the particle counts are higher than the number of particles shown in Figures 7 and 8. Whereas Figure 7a,b demonstrates the state of the samples obtained after electrodeposition at -0.54 mA/cm^2 for 10 and 20 s, Figure 8a,b shows the results of electrodeposition at -1.1 mA/cm^2 for 10 and 20 s. Comparison of Figures 7 and 8 at corresponding electrodeposition times indicates that the particle density increases with current density (or overpotential). This result is consistent with previous observations that the nucleation density exponentially increases with overpotential.[11−13] The exponential dependence is due to a distribution of activation energies associated with nucleation sites.[11]

The effect of electrodeposition time on the particle density and particle diameter is determined from examination of Figures 7a,b and 8a,b. Table 1 shows that mean particle diameters increase with the electrodeposition time. The particle densities for samples prepared at cathodic current densities of 0.54 and 1.1 mA/cm^2 are 2×10^6 and 5×10^6 particles/cm^2, respectively. Lower particle densities of $(1-5) \times 10^5$ particles/cm^2 were obtained with cathodic current densities of $0.07-0.18$ mA/cm^2. Analysis of micrographs and histograms allows us to conclude the following. First, at a given current density, the particle density remains almost constant as the electrodeposition proceeds over the investigated period of time. Second, for a given sample the distribution of particle diameters is comparatively narrow, with the relative standard deviation being approximately 25%. These two observations indicate that nucleation occurs only at the onset of the deposition process. Thus, electrodeposition proceeds by the instantaneous nucleation mechanism.[13]

Our experimental observations do not allow us to clearly discriminate whether the growth of gold particles proceeds under kinetic or diffusion control. The absence of a diffusion-limited peak in CV results (Figure 1a) indirectly suggests that growth of particles is kinetically limited. However, the presence of this peak could be masked by an onset of water electrolysis. For the same reason, potential step experiments from OCP to 0.4−0.5 V more negative potentials resulted in current−time curves in which electrodeposition current monotonically became more negative (after the charging current decayed to zero). Chronoamperometric experiments are frequently used to investigate the growth of particles.[12,13,24−26] Under conditions of diffusion control, the cathodic electrodeposition current reaches the most negative value and then becomes less negative because of diffusion limitations. We also note that more complex nucleation and growth mechanism(s) was (were) present at longer electrodeposition times. Under these conditions, we observed higher particle densities, broad distributions of particle diameters, and coalescence of neighboring particles. However, these limitations did not prevent us from establishing the mechanism of nucleation at short deposition times. In this case, a combination of instantaneous nucleation, low particle densities (10^5-10^7 particles cm^{-2}), and possible kinetic control of electrodeposition favored the conditions under which the overlap of diffusion zones around individual particles during electrodeposition was

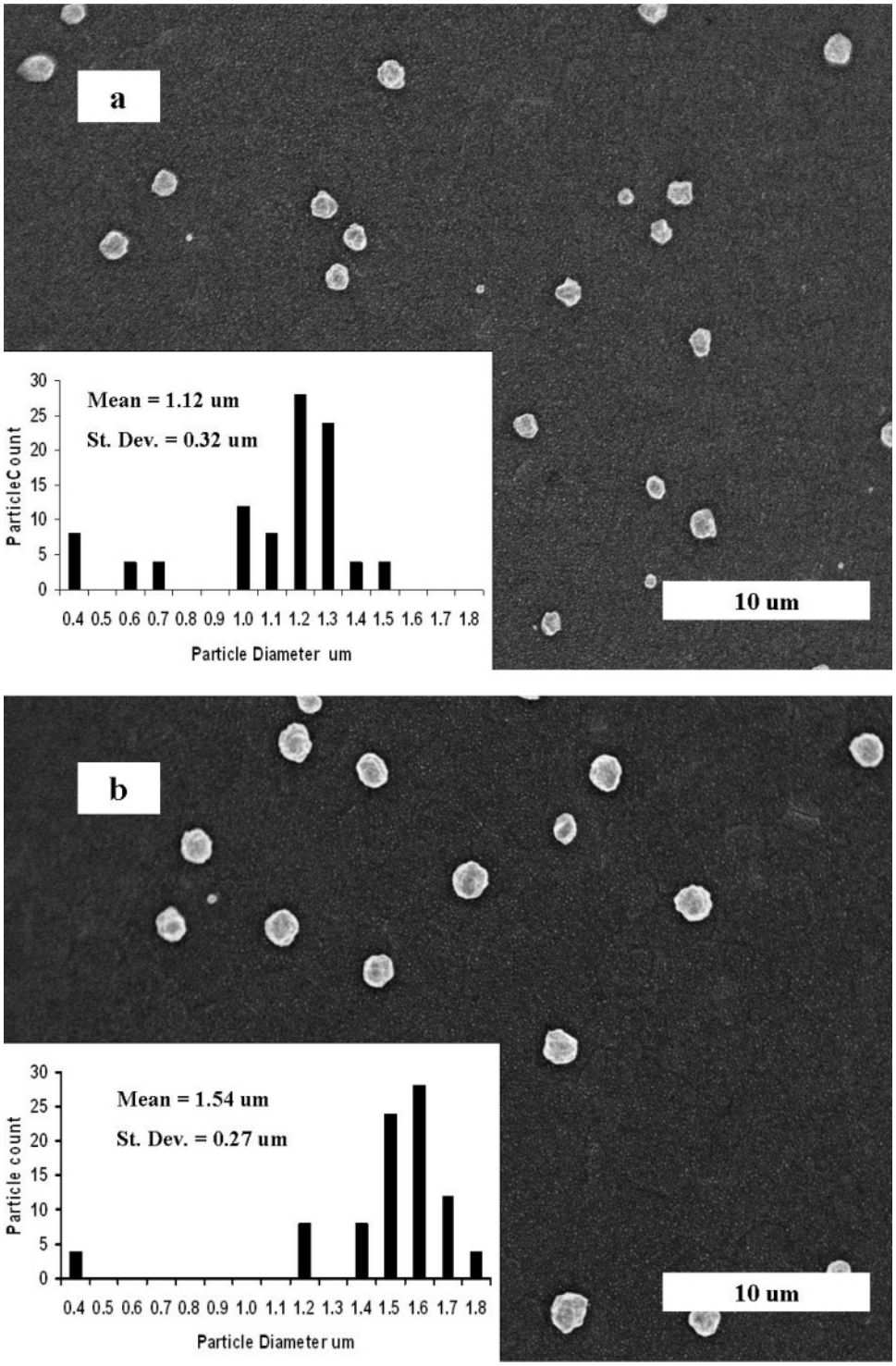

Figure 7. SEM micrographs obtained after electrodeposition at −0.54 mA/cm^2 for (a) 10 and (b) 20 s.

almost negligible.[13] As a result, electrodeposition produced particles with a relatively narrow distribution of diameters.

Gold electrodeposition can be compared with previously reported electroless deposition of silver on the aluminum/copper substrate.[10] In a dramatic contrast to electroless deposition, the electrodeposition of gold allows control of both the particle density and particle diameter. Whereas the former is determined by the overpotential and the latter is controlled by the electrodeposition time. Therefore, electrodeposition is the method of choice for fabrication of particle-type films with a controlled particle density and a narrow distribution of particle diameters.

In addition to elucidating the mechanism of nucleation, it is important to address the role of the substrate pretreatment for the subsequent deposition of gold particles. The two pretreatment processes, namely, anodization of aluminum/copper films and the following etching of the aluminum oxide, make the electrodeposition of gold possible. It can be speculated that, under our processing conditions, copper becomes preconcentrated on the surface of the substrate. Enrichment of copper just beneath the film of anodic aluminum oxide was observed during anodization of Al/Cu alloys.[44−47] In addition, aluminum oxide was reported to dissolve more readily than copper in acidic media.[48] Thus, aluminum oxide could be selectively dissolved

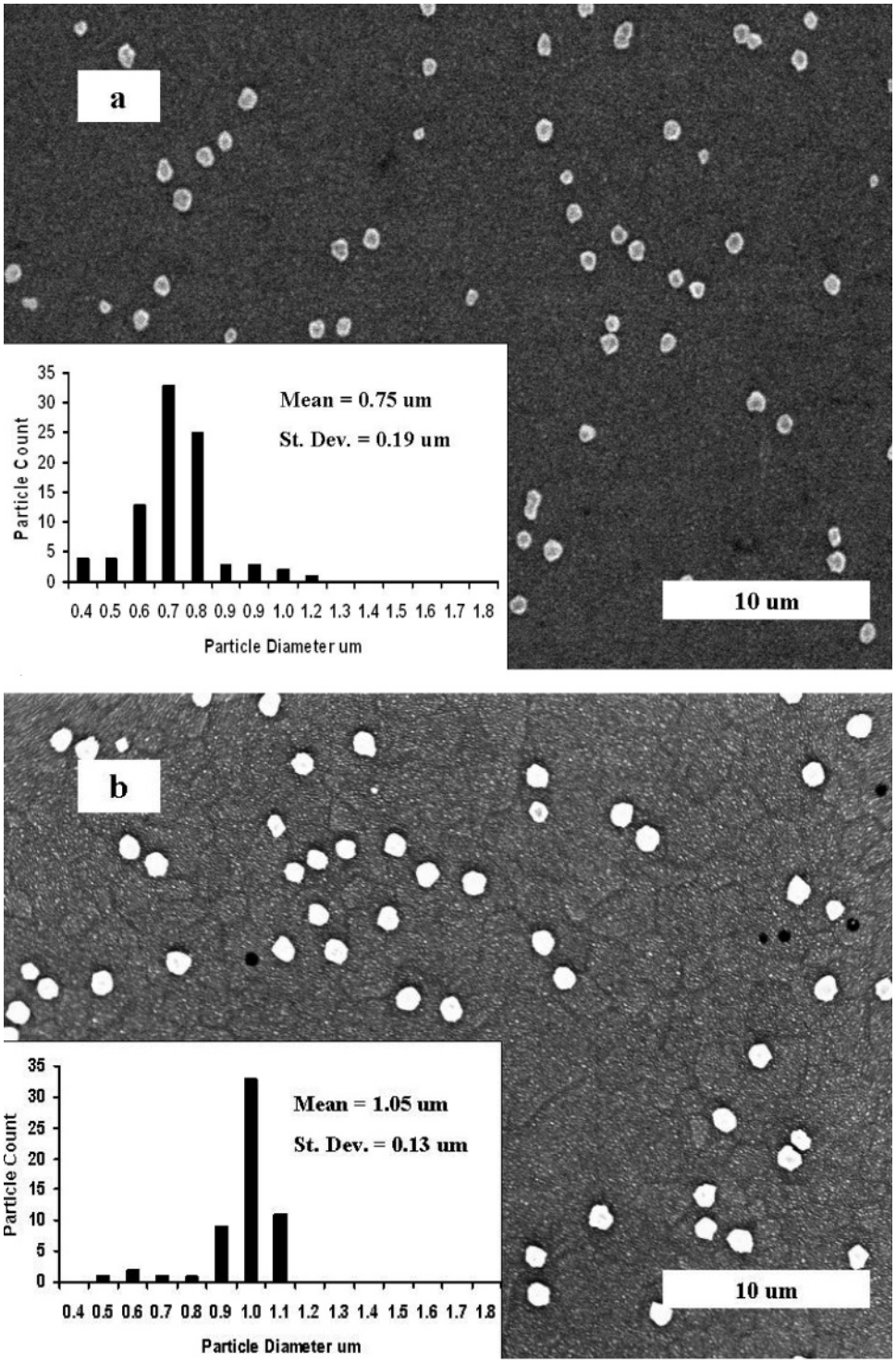

Figure 8. SEM micrographs obtained after electrodeposition at −1.1 mA/cm^2 for (a) 10 and (b) 20 s.

TABLE 1: Mean Particle Diameters (μm) for Electrodeposition Times and Current Densities Shown in Figures 7 and 8

	current density (mA/cm^2)	
time (s)	0.54	1.1
10	1.1 ± 0.3	0.75 ± 0.19
20	1.5 ± 0.3	1.1 ± 0.3

during etching. In another study, electroless deposition of Cu and Pd on annealed aluminum/copper films of similar compositions were described.[49] In this case, the depth profiling by X-ray photoelectron spectroscopy showed that thermal annealing at 400 °C increased the copper concentration near the surface and allowed for metal deposition in a manner similar to that reported here. Further, gold electrodeposition on copper substrates is possible, as reported elsewhere.[50,51] Thus, enrichment of copper in and/or underneath the layer of barrier aluminum oxide during anodization and etching might result in facile electrodeposition of gold on aluminum/copper films.

The EIS data (Figure 4) indicate that gold particles are electrically connected to the underlying aluminum/copper film. To verify the electrical connectivity, we performed CV experiments with a soluble redox couple, $Ru(NH_3)_6^{3+}$ (0.5 mM) in 0.5 M phosphate buffer (pH 7). A redox couple with a sufficient negative formal potential of about −0.23 V (Ag/AgCl) was

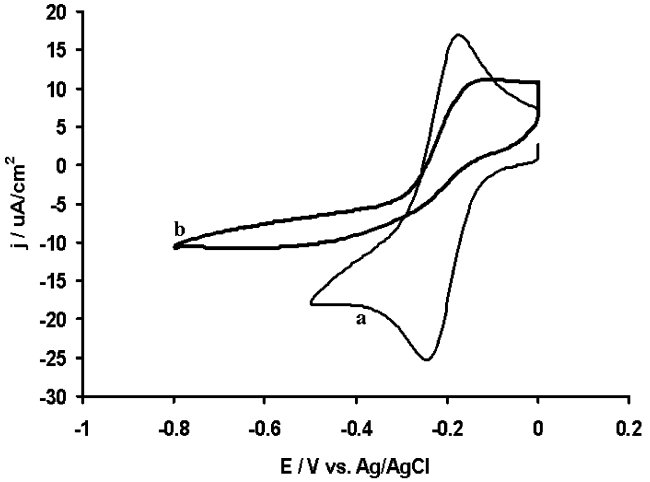

Figure 9. Cyclic voltammograms (10 mV/s) of 0.5 mM $Ru(NH_3)_6^{3+}$ in 0.5 M phosphate buffer: (a) bare gold electrode and (b) processed wafer with gold particles.

chosen to avoid the application of potentials that can result in oxidation of copper incorporated in and/or underneath the layer of barrier aluminum oxide. Figure 9 shows the voltammograms obtained for two electrodes: (a) an evaporated gold electrode and (b) aluminum/copper film with deposited gold particles, both having the same geometric area. Substrate b was obtained after 40 s of electrodeposition at the current density of -0.018 mA/cm^2. These conditions favored the formation of gold particles with a low density and a high ratio between the interparticle distance and particle diameter. The evaporated gold electrode demonstrates the typical faradaic response for a reversible redox couple with the peak separation of about 60 mV.[40] At the same time, the CV curve for the aluminum/copper film with gold particles resembles a sigmoidal shape. This shape results from a superposition of two responses: one characteristic for semi-infinite diffusion (as in the case of evaporated gold) and the other characteristic for semi-spherical diffusion to the individual gold particles.[40] At the time scale of CV experiments (10 mV/s), a low particle density results in only a partial overlap among diffusion zones formed around gold particles. Therefore, the CV curve for $Ru(NH_3)_6^{3+}$ at the aluminum/ copper electrode with gold particles is a combination of two responses. In summary, these electrochemical experiments support that electrodeposition produces gold particles that are electrically connected to the aluminum/copper substrate. In addition, they mimic the electrochemical behavior associated with an array of microelectrodes.

Conclusions

We report a procedure for the electrodeposition of gold particles on films containing 99.5% aluminum and 0.5% copper. Activation of aluminum/copper films is accomplished by anodization and subsequent chemical etching of aluminum oxide. These processes result in copper enrichment in and/or underneath the layer of barrier aluminum oxide. This procedure for substrate pretreatment can be used as an alternative to the traditionally used zincate process for electrodeposition on aluminum. Electrodeposition on aluminum/copper films results in the formation of gold particles. Analysis of the EIS data indicates that the deposited gold particles increase the interfacial capacitance and decrease the resistance connected in parallel to the interfacial capacitance. Evaluation of the micrographs suggests that electrodeposition proceeds by instantaneous nucleation followed by three-dimensional growth of semispherical particles. A combination of instantaneous nucleation, low particle densities (10^5-10^7 particles cm^{-2}), and possible kinetic control of electrodeposition favored the formation of gold particles with a relatively narrow distribution of diameters. Whereas the particle density is determined by the overpotential, the particle diameter is controlled by the electrodeposition time. Therefore, electrodeposition is the method of choice for the fabrication of particle-type films with a controlled particle density and a narrow size distribution. The gold particles are electrically connected to the aluminum/copper substrate. As a result, the aluminum/copper film with gold particles shows a reversible faradaic response for $Ru(NH_3)_6^{3+}$. The electrochemical response is similar to one associated with an array of microelectrodes. The fabricated films of gold particles with a control particle density and diameter distribution can be utilized in a number of applications, including catalysis, electrocatalysis, and optical and electronic devices.

Acknowledgment. This work was supported by DOE/ WERC of New Mexico and the Center for Micro-Engineered Materials (UNM). The SEM laboratory was supported by the New Mexico EPCoR NSF grant and the NNIN grant. We thank Todd M. Bauer (Sandia National Laboratories, Albuquerque, NM) for assistance with fabrication of silicon wafers with an aluminum/copper layer and Geoff Courtin (UNM) for assistance with processing of micrographs.

References and Notes

(1) Robertson, S. G.; Ritchie, I. M.; Druskovich, D. M. *J. Appl. Electrochem.* **1995**, *25*, 659.
(2) Pearson, T.; Wake, S. J. *Trans. Inst. Met. Finish.* **1997**, *75* (3), 93.
(3) Lashmore, D. S. *Plat. Surf. Finish.* **1978**, *65*, 44.
(4) Stoyanova, E.; Stoychev, D. *J. Appl. Electrochem.* **1997**, *27*, 685.
(5) Court, S. W.; Baker, B. D.; Walsh, F. C. *Trans. Inst. Met. Finish.* **2000**, *78* (4), 157.
(6) Hutt, D. A.; Liu, C.; Conway, P. P.; Whalley, D. C.; Mannan, S. H. *IEEE Trans. Compon., Packag. Technol.* **2002**, *25* (1), 87.
(7) Watanabe, H.; Honma, H. *J. Electrochem. Soc.* **1997**, *144* (2), 471.
(8) Bettelheim, A.; Raveh, A.; Mor, U.; Ydgar, R.; Segal, B. *J. Electrochem. Soc.* **1990**, *137* (10), 3151.
(9) Fang, R.; Gu, H.; O'Keefe, M. J.; O'Keefe, T. J.; Shih, W. S.; Leedy, K. D.; Cortez, R. *Elect. Mater.* **2001**, *30* (4), 349.
(10) Brevnov, D. A.; Olson, T. S.; López, G. P.; Atanassov, P. *J. Phys. Chem. B* **2004**, *108* (45), 17531.
(11) Budevski, E.; Staikov, G.; Lorenz, W. J. *Electrochim. Acta* **2000**, *45* (15−16), 2559.
(12) Oskam, G.; Long, J. G.; Natarajan, A.; Searson, P. C. *J. Phys. D: Appl. Phys.* **1998**, *31* (16), 1927.
(13) Penner, R. M. *J. Phys. Chem. B* **2002**, *106* (13), 3339.
(14) Oskam, G.; Searson, P. C. *J. Electrochem. Soc.* **2000**, *147* (6), 2199.
(15) Ji, C. X.; Oskam, G.; Serson, P. C. *J. Electrochem. Soc.* **2001**, *148* (11), C746.
(16) Radisic, A.; Cao, Y.; Taephaisitphongse, P.; West, A. C.; Searson, P. C. *J. Electrochem. Soc.* **2003**, *150* (5), C362.
(17) Radisic, A.; Oskam, G.; Searson, P. C. *J. Electrochem. Soc.* **2004**, *151* (6), C369.
(18) Zoval, J. V.; Stiger, R. M.; Biernacki, P. R.; Penner, R. M. *J. Phys. Chem.* **1996**, *100* (2), 837.
(19) Zoval, J. V.; Lee, J.; Gorer, S.; Penner, R. M. *J. Phys. Chem. B* **1998**, *102* (7), 1166.
(20) Marquez, K.; Staikov, G.; Schultze, J. W. *Trans. Inst. Met. Finish.* **2002**, *80* (13), 73.
(21) Krumm, R.; Guel, B.; Schmitz, C.; Staikov, G. *Electrochim. Acta* **2000**, *45* (20), 3255.
(22) Milchev, A.; Stoychev, D.; Lazarov, V.; Papoutsis, A.; Kokkinidis, G. *J. Cryst. Growth* **2001**, *226* (1), 138.
(23) Harrison, J. A. *J. Electroanal. Chem.* **1972**, *36*, 71.
(24) Gunawrdena, G.; Hills, G.; Montenegro, I.; Scharifker, B. *J. Electroanal. Chem.* **1982**, *138*, 225.
(25) Gunawrdena, G.; Hills, G.; Montenegro, I. *J. Electroanal. Chem.* **1982**, *138*, 241.
(26) Scharifker, B.; Hills, G. *Electrochim. Acta* **1983**, *28* (7), 879.
(27) Ueda, M.; Dietz, H.; Anders, A.; Kneppe, H.; Meixner, A.; Plieth, W. *Electrochim. Acta* **2002**, *48* (4), 377.
(28) Zheng, M.; West, A. C. *J. Electrochem. Soc.* **2004**, *151* (7), C502.

(29) Maye, M. M.; Lou, Y.; Zhong, C.-J. *Langmuir* **2000**, *16*, 7520.
(30) Brankovic S. R.; Wang J. X.; Adzic R. R. *Electrochem. Solid-State Lett.* **2001**, *4* (12), A217.
(31) Zhang, Y. R.; Asahina, S.; Yoshihara, S.; Shirakashi, T. *Electrochim. Acta* **2003**, *48* (6), 741.
(32) Chan, K. Y.; Ding, J.; Ren, J. W.; Cheng, S. A.; Tsang, K. Y. *J. Mater. Chem.* **2004**, *14* (4), 505.
(33) Cherstiouk, O. V.; Simonov, P. A.; Savinova, E. R. *Electrochim. Acta* **2003**, *48* (25−26), 3851.
(34) Haruta, M.; Yamada, N.; Kobayashi, T.; Iijima, S. *J. Catal.* **1989**, *115*, 301.
(35) Haruta, M.; Tsubota, S.; Kobayashi, T.; Kageyama, H.; Genet, M. J.; Delmon, B. *J. Catal.* **1993**, *144*, 175.
(36) El-Deab, M.; Okajima, T.; Ohsaka, T. *J. Electrochem. Soc.* **2003**, *150* (7), A851.
(37) Daniel, M. C.; Astruc, D. *Chem. Rev.* **2004**, *104* (1), 293.
(38) Roy, D.; Fendler, J. *Adv. Mat.* **2004**, *16* (6), 479.
(39) Gupta, R.; Dyer, M. J.; Weimer, W. A. J. *Appl. Phys.* **2002**, *92* (9), 5264.
(40) Bard, A. J.; Faulkner, L. R. *Electrochemical Methods: Fundamentals and Applications*; John Wiley: New York, 1980.
(41) Bard, A. J.; Parsons, R.; Jordan, J. *Standard Potentials in Aqueous Solution*; Marcel Dekker Inc.: New York, 1985.
(42) Brevnov, D. A.; Rama Rao, G. V.; Lopez, G. P.; Atanassov, P. B. *Electrochim. Acta* **2004**, *49* (15), 2487.
(43) Menon, V. P.; Martin, C. R. *Anal. Chem.* **1995**, *67*, 1920.
(44) Strehblow, H. H.; Melliar-Smith, C. M.; Augustyniak, W. M. *J. Electrochem. Soc.* **1978**, *125*, 915.
(45) Habazaki, H.; Zhou, X.; Shimizu, K.; Skeldon, P.; Thompson, G. E.; Wood, G. C. *Electrochim. Acta* **1997**, *42* (17), 2627.
(46) Habazaki, H.; Shimizi, K.; Skeldon, P.; Thompson, G. E.; Wood, G. C.; Zhou, X. *Trans. Inst. Met. Finish.* **1997**, *75* (1), 18.
(47) Paez, M. A.; Bustos, O.; Thompson, G. E.; Skeldon, P.; Shimizu, K.; Wood, G. C. *J. Electrochem. Soc.* **2000**, *147* (3), 1015.
(48) Kolics, A.; Besing, A. S.; Wieckowski, A. *J. Electrochem. Soc.* **2001**, *148* (8), B322.
(49) O'Keefe, M. J.; Leedy, K. D.; Grant, J. T.; Fang, M.; Gu, H.; O'Keefe, T. J. *J. Vac. Sci. Technol. B* **1999**, *17* (5), 2366.
(50) Rao, S. T.; Weil, R. *J. Electrochem. Soc.* **1980**, *127* (5), 1030.
(51) Li, Y. G.; Lasia, A. *J. Appl. Electrochem.* **1997**, *27*, 643.